Research in Astron. Astrophys. **2011** Vol. **11** No. **12**, 1469–1481
http://www.raa-journal.org *http://www.iop.org/journals/raa*

Research in Astronomy and Astrophysics

CCD photometry of W UMa-type contact binaries in the old open cluster Berkeley 39

Yellapragada Ravi Kiron[1], Kandulapati Sriram[2] and Pasagada Vivekananda Rao[1]

[1] Department of Astronomy, Osmania University, Hyderabad 500 007, India; *yravikiron@yahoo.com*
[2] Korea Astronomy and Space Science Institute, Hwaam 61-1, Yuseong, Daejeon 305-348, South Korea

Received 2011 June 7; accepted 2011 August 29

Abstract We present the combined BVI multicolor photometric solutions of seven EW variables in the old open cluster Berkeley 39. The observations were carried out in the B and V passbands from the 2 m telescope at the IUCAA-Girawali Observatory in India. The analysis is done using the 2003 version of the Wilson-Devinney code and the fitted light curves are presented. The light curves appear to be symmetric in all the passbands. The photometric solutions suggest that the variables are W-type systems. The new ephemeris indicates that the orbital periods of the studied variables have not changed during the timespan of observations. Revised orbital period, absolute mass, radius and luminosity of the respective variables are presented. The absolute physical parameters of the variables follow the trend of field EW stars. Comparing the results obtained with the other theoretical works, we suggest that there is an excess loss of mass and angular momentum in these systems which may be due to their short period and relatively young age, possibly due to the presence of a third component or the initial detached period being less than 2 d.

Key words: binaries — eclipsing: contact: W UMa stars

1 INTRODUCTION

Berkeley 39 (Be39) is a rich old open cluster located in the direction of the galactic anticenter. The central coordinates of the cluster are $(\alpha_{\rm J2000} = 07^{\rm h}44^{\rm m}, \delta_{\rm J2000} = -04°36')$. Kaluzny et al. (1993) and Mazur et al. (1999) discovered more than 17 variables, of which 12 were found to be EW type. Based on the study of the Color Magnitude Diagram (CMD), Girardi & Bertelli (1998) obtained the age of Be39 to be around 6 ± 1 Gyr. However, by applying theoretical and recent observational constraints, Percival & Salaris (2003) found the age to be around 7.5 ± 1 Gyr. On the basis of the spectroscopic study, Janes et al. (1992) derived [Fe/H]$= -0.31 \pm 0.08$ for the metallicity of Be39. Percival & Salaris (2003) found the de-reddened distance modulus to be 12.97 ± 0.09 along with the metallicity [Fe/H]$= -0.15 \pm 0.09$. The properties of Be39 and the photometric solutions of variables $V1, V4, V7$ and $V8$[1] in the I passband were discussed in Sriram et al. (2009).

[1] As per the nomenclature of Kaluzny et al. (1993).

Contact binaries are short-period eclipsing variables broadly classified into A- or W-type on the basis of their light curve (Binnendijk 1970). Earlier studies (Hilditch 1989) suggested that A-type stars are relatively more evolved than the W-type ones but this scenario is ruled out by the fact that A-type stars have high total mass and angular momentum (AM) compared to what is generally found in W-types (Gazeas & Niarchos 2006). Despite the slight but vivid physical distinction in the evolution among A- and W-types, Gazeas & Stępień (2008) showed that these systems ultimately merge and form a single fast-rotating star. Li et al. (2008) suggested that during their dynamical evolution these systems should have a low mass ratio. Jiang et al. (2010) found that the minimum mass ratio of contact binaries decreases with increasing mass of the primary if the primary mass is $\leq 1.3\,M_{\odot}$, but above this mass the ratio is roughly constant. However they found that it is difficult to determine whether the next evolutionary stage of these systems is to become a fast-rotating star or if they evolve into a high mass ratio system through the process of thermal relaxation oscillation (TRO).

Large numbers of contact binaries have been discovered in open and globular clusters (Rucinski 1998, 2000 and references therein). The observations of binaries in an open cluster provide us with important astrophysical tools to estimate the distance to the cluster and various evolutionary phases of binaries themselves. Rucinski (1993) found their relative frequencies of occurrence seem to be much higher than the field stars, indicating action of multi-body collision processes, possibly intertwined with nuclear and angular-momentum evolution of individual components. Predicting the evolution of these W UMa-type systems in clusters may help in understanding the formation of blue stragglers.

Since the B and V passband observations were lacking for the variables in Be39, we carried out an observation campaign on this cluster. The EW variable stars that we could find in the frame of $10.5' \times 10.5'$ are V1, V2, V6, V7, V8, V10 and V11. In our study, we consider component 1 as the higher temperature star and component 2 as the lower temperature star.

2 OBSERVATIONS AND DATA REDUCTION

The observations of open cluster Be39 were carried out from the IUCAA-Girawali Observatory (IGO) using the 2 meter telescope. The observations in the B and V passbands were carried out in two allotted cycles, during 2009 January 19–21 and February 04–08. The CCD used for imaging provided an effective field of view of $10.5' \times 10.5'$ on the sky corresponding to a plate scale of 0.3 arcsec pixel^{-1}. The full width at half maximum (FWHM) of the stellar image varied from $3-5$ pixels during the observations. A brief description of the telescope's instruments can be found in Sriram & Vivekananda Rao (2010). As per Mazur et al. (1999), the apparent $V_{\rm max}$ magnitudes for the variables are viz V1 15.40, V2 16.13, V6 17.98, V7 18.38, V8 19.03, V10 15.89 and V11 19.67. Considering the magnitude range, during the observations, the exposure time was set to 600 s for both the bands and the observations were taken with the field centered at $\alpha_{\rm J2000} = 07^{\rm h}44^{\rm m}, \delta_{\rm J2000} = -04°36'$. For the selection of the comparison star (C1) and the check star (C2), we have chosen several stars which are relatively bright.

Figure 1 shows the positions of the variable stars, the comparison star and the check star. It was found that the magnitude of the comparison star with the co-ordinates $\alpha_{\rm J2000} = 07^{\rm h}46^{\rm m}54^{\rm s}$, $\delta_{\rm J2000} = -4°42'22''$ remained constant during the period of our observations. The difference of magnitudes between the comparison and check stars for eight observing nights in the B and V filters are shown in Figure 2. It was found that the difference in magnitude between C1 and C2 stars was constant in brightness with a probable error of $\pm$0.004 mag for the V and $\pm$0.006 mag for the B band. The cluster was observed at various air-mass values ranging from 1.1–2.0. In total, for both the B and V passbands, 194 frames were obtained for variables V1, V2 and V10 and 168 frames for variables V6, V7 and V8, as well as 158 frames for V11. We carried out differential photometry and the extinction corrections were ignored for magnitude and color calibrations.

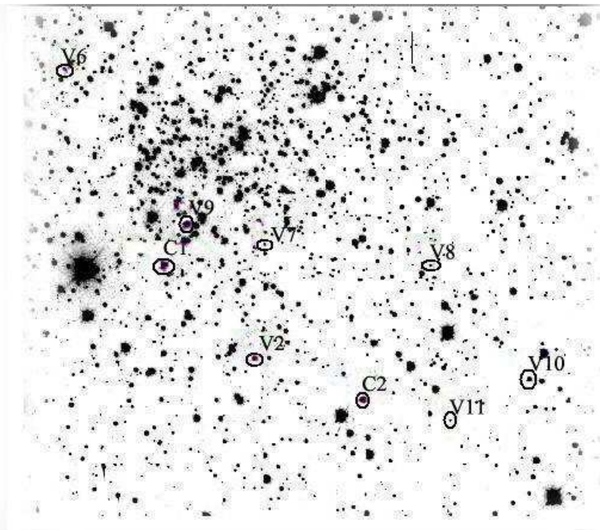

Fig. 1 $10' \times 10'$ image of the field of Be39. The range of R.A. along the horizontal axis is $07^{\rm h}47^{\rm m}20^{\rm s}$, $07^{\rm h}46^{\rm m}40^{\rm s}$ and that of Dec is $-04°37'$, $-04°47'$. The center of the field is $07^{\rm h}47^{\rm m}00^{\rm s}$, $-04°42'$. The variables are labeled along with check and comparison stars.

We performed aperture photometry with the *apphot* package available in the IRAF[2] software. Using a circular aperture of an arbitrary radius (depending on the sources) that encloses the sources, we determined the number of counts within this aperture. An annular ring of much larger radius and width of about 5 pixels was used to estimate the background counts. The background counts were subtracted from the counts measured within the aperture to get the variable counts and thus the instrumental magnitudes were obtained. The probable errors that were obtained for the brightest variable V1 are ± 0.006 mag in the B passband, and ± 0.004 mag in the V passband, and for the faintest variable V11 are ± 0.023 mag in the B passband and ± 0.019 mag in the V passband.

Due to the variations in the sky conditions, we could not calibrate the apparent magnitudes. However, the differential magnitudes were obtained for the variable stars by subtracting the magnitude of the variable star from the magnitude of the comparison star. The Heliocentric Julian Dates (HJD) were obtained from the time of observation. The phases of the variables were calculated using their periods (discussed in the next section). Using the data obtained by us in the B and V passbands and the set of I passband data from Kaluzny et al. (1993), we derived the combined multicolor photometric solutions for each variable.

3 PERIOD ANALYSIS AND DETERMINATION OF EPHEMERIS

The times of minima (Table 1) were determined from the data using the method of Kwee & van Woerden (1956). The revised epoch and period of each variable studied in the present work are derived from the observed times of minima. Table 2 (cols. 2 and 3) shows the result of new epochs and periods. Using the new epoch and period, eclipse timing residuals are calculated. It is found that the residuals do not show any significant variation, indicating that the period has remained constant during the years 1993 to 2009 for the observed binaries.

[2] IRAF is distributed by the National Optical Astronomy Observatory, which is operated by the Association of Universities for Research in Astronomy (AURA) under cooperative agreement with the National Science Foundation.

Table 1 CCD Times of Light Minima for the Observed Variables of Be39

Variable	J.D. Hel.	Min.	E	(O-C)	Origin
V1	2448285.7930	I	−16250	0.0031	Kaluzny et al. (1993)
	2454851.2435	I	−47	−0.0025	This paper
	2454852.2593	II	−44.5	0.0008	This paper
	2454853.2796	I	−42	0.0081	This paper
	2454866.2429	I	−10	0.005	This paper
	2454867.2567	II	−7.5	0.0058	This paper
	2454868.2704	I	−5	0.0065	This paper
	2454869.2850	II	−2.5	0.0081	This paper
	2454870.2899	I	0	0	This paper
V2	2448285.8060	II	−13497.5	0.00375	Kaluzny et al. (1993)
	2454851.3674	I	−2	−0.0031	This paper
	2454852.3435	I	0	0	This paper
	2454853.3168	I	2	0.0003	This paper
	2454866.2071	II	28.5	−0.00165	This paper
	2454867.1772	II	30.5	−0.00455	This paper
	2454868.1495	II	32.5	−0.00525	This paper
	2454869.3707	I	35	−0.0003	This paper
	2454870.3370	I	37	−0.007	This paper
V6	2448226.9810	I	−23299	0.0019	Kaluzny et al. (1993)
	2454851.2332	I	−7	0.0093	This paper
	2454851.3658	II	−6.5	−0.0003	This paper
	2454852.2234	II	−3.5	0.0041	This paper
	2454852.3647	I	−3	0.0032	This paper
	2454853.2147	I	0	0	This paper
	2454853.9379	II	2.5	0.0122	This paper
	2454866.2989	I	46	0.0018	This paper
	2454867.1554	I	49	0.0051	This paper
	2454867.3005	II	49.5	0.008	This paper
	2454868.1418	II	52.5	−0.0039	This paper
	2454868.2880	I	53	0.0001	This paper
	2454869.1418	I	56	0.0007	This paper
	2454869.2848	II	56.5	0.0015	This paper
V7	2448226.8850	I	−23893	0.0042	Kaluzny et al. (1993)
	2454851.2087	II	−64.5	0.0049	This paper
	2454852.3185	II	−60.5	0.0027	This paper
	2454853.2870	I	−57	−0.0018	This paper
	2454866.3592	I	−10	0.0044	This paper
	2454867.3353	II	−6.5	0.0075	This paper
	2454868.3033	I	−3	0.0025	This paper
	2454869.1348	I	0	0	This paper
	2454869.2783	II	0.5	0.0045	This paper
V8	2448226.7640	II	−29031.5	-2.5×10^{-10}	Kaluzny et al. (1993)
	2454851.3234	I	−78	−0.0014	This paper
	2454852.2402	I	−74	0.0002	This paper
	2454852.3516	II	−73.5	−0.0028	This paper
	2454853.2696	II	−69.5	1.71×10^{-11}	This paper
	2454853.3826	I	−69	−0.0014	This paper
	2454866.3109	II	−12.5	−0.0003	This paper
	2454867.3397	I	−8	−0.0011	This paper
	2454869.1712	I	0	0	This paper
	2454869.2832	II	0.5	−0.0024	This paper
V10	2448226.8550	II	−12257.5	−0.02205	Kaluzny et al. (1993)
	2454851.0627	II	−33.5	−0.00038	This paper
	2454852.1471	II	−31.5	0.00045	This paper
	2454853.5012	I	−29	−0.0004	This paper
	2454866.2362	II	−5.5	0.00055	This paper
	2454867.3203	II	−3.5	5×10^{-5}	This paper
	2454869.2163	I	0	0.0004	This paper
	2454870.3118	I	2	0.0117	This paper

Table 1 — *Continued.*

Variable	J.D. Hel.	Min.	E	(O-C)	Origin
V11	2454851.2978	II	−8.5	5×10^{-5}	This paper
	2454851.4042	I	−8	1×10^{-4}	This paper
	2454852.1974	II	−4.5	0.00015	This paper
	2454852.4288	II	−3.5	0.00615	This paper
	2454853.2147	I	0	0	This paper
	2454853.3315	II	0.5	0.00365	This paper
	2454866.3405	I	58	0.0001	This paper
	2454867.2452	I	62	−0.0002	This paper
	2454868.1506	I	66	−0.0005	This paper
	2454868.3773	I	67	0.0001	This paper

Table 2 Epoch and Period for Each Variable

Variable	Epoch (JD Hel.)	Period (d)
V1	2454870.2939(40)	0.4052000(35)
V2	2454852.3408(42)	0.4865001(36)
V6	2454853.2179(43)	0.2844001(28)
V7	2454869.1379(39)	0.2779995(37)
V8	2454869.1702(41)	0.2287999(39)
V10	2454869.2182(42)	0.5419019(32)
V11	2454853.2151(44)	0.2262967(39)

4 PHOTOMETRIC SOLUTIONS

BVI combined photometric solutions were obtained using the 2003 version of the Wilson-Devinney (WD) code with an option of non-linear limb darkening via a square root law along with many other features (Wilson & Devinney 1971; van Hamme & Wilson 2003). The visual inspection of these variables indicates the W UMa contact binary nature, and hence mode 3 was used. The effective temperature for the primary component T_1 was obtained from the average de-reddened $(B-V)$ values for the variables (Mazur et al. 1999), and using the tables given by Allen & Cox (2000). The initial value for the effective temperature of the secondary component T_2 was assumed to be slightly less than T_1 and it was kept as a free parameter.

Because of the convective nature of heat transportation in envelopes, the gravity darkening exponents for the system are taken as $g_1 = g_2$ = 0.32 (Lucy 1967). Assuming circular orbits, the eccentricity *e* is fixed at 0. From Ruciński (1969), the values of the bolometric albedo $A_1 = A_2$ are fixed at 0.5. The rotation and revolution for the variable are assumed to be synchronized, hence we chose F1=F2=1. The values of the limb darkening coefficients of components x_1, x_2 are taken as 0.610 and 0.549 (Diaz-Cordoves et al. 1995) for the B and V passbands respectively. The wavelengths are taken as 4455 Å and 5497 Å for the B and V passbands respectively. The adopted adjustable parameters are: the orbital inclination (i), the temperature of secondary component T_2, the dimensionless potential of the primary star Ω_1 and the monochromatic luminosity of the primary star L_1. Since no spectroscopic observations are available for the variables, we used the q search method to constrain the most important parameter, the mass ratio $q\ (= m_2/m_1)$. In order to find the best value of the mass ratio, we executed the differential code (DC) for various assumed values of mass ratio, while keeping in mind that the surface potential $(\Omega_1 = \Omega_2)$ also changes with respect to the mass ratio. The corresponding value for the surface potential Ω_1 was calculated using the equation given by Kopal (1959). To obtain the best value of mass ratio, we assumed a series of values of q (from 0.3 – 4.0 with a stepwise increase of 0.1). The resulting sum $\sum \omega_i (\mathrm{O}-\mathrm{C})_i^2$ of the weighted square deviations of the converged solutions for each value is shown in Figure 3. Finally we executed the program,

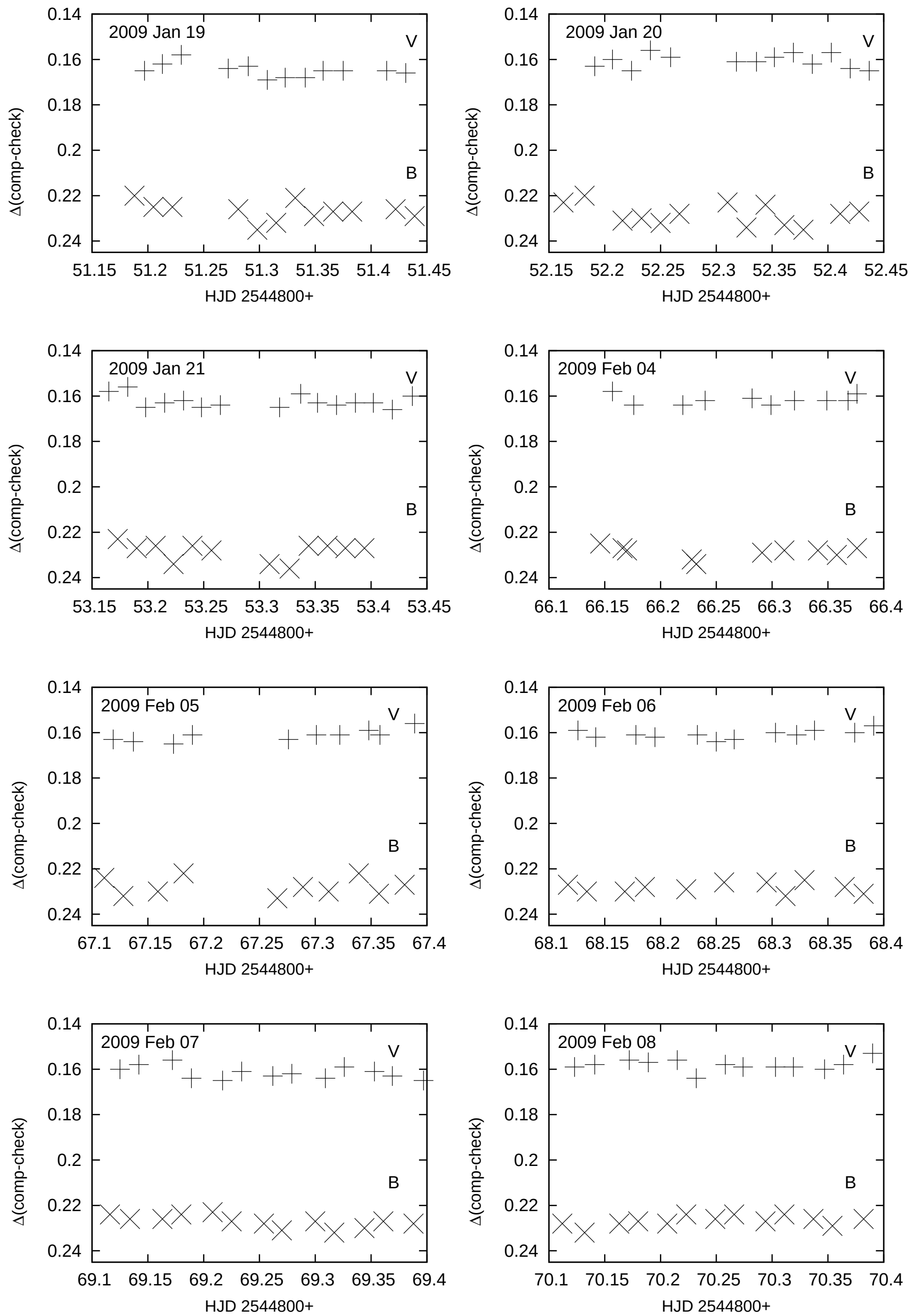

Fig. 2 Eight panels show the magnitude differences in the B and V passbands between the comparison and check stars versus HJD for observations on 2009 January 19–21 and February 04–08.

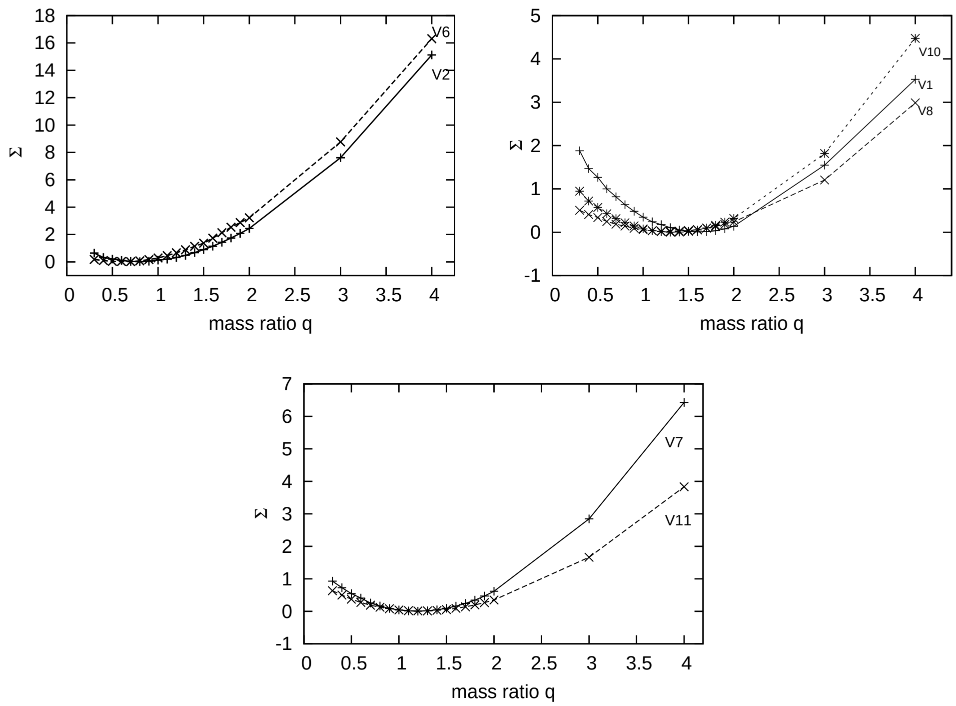

Fig. 3 Mass ratio (q) versus sigma ($\sum$) plot using the combined multi-color passband data for each variable.

freeing the parameter mass ratio and inclination along with other free parameters viz. inclination (i), secondary component temperature (T_2), surface potential (Ω_1) and monochromatic luminosity of the primary component (L_1). The results of the final analysis are shown in Table 3. From these parameters, theoretical light curves were computed using the light curve (LC) code (Figs. 4, 5 and 6). We find that the scatter is much less in the B and V passbands compared to the I passband.

5 RESULTS

For the observed variables, the absolute magnitude M_V is obtained from the relation $M_V = -4.44 \log P + 3.02(B-V)_o + 0.12$ (Rucinski & Duerbeck 1997). The apparent magnitude m and $E(B-V) = 0.15$ are taken from Mazur et al. (1999) and using the distance modulus equation $m - M_V = 5 \log d - 5$, the distance d is derived. The results of each of the systems are discussed below:

5.1 Variable V1

The period of the system is $0.4052\mathrm{d}$ and $B-V = 0.51$, which closely corresponds to the G0 spectral type. The combined result in the three bands shows a temperature difference of $\sim 235\,\mathrm{K}$ between the two components. The best combined values of q and i are 1.72 and $67°$ respectively. The fill-out factor is 0.163 which is of intermediate level. The distance of the variable is around $2512\,\mathrm{pc}$. This distance indicates that this variable is not a member of the cluster and it is a foreground field star.

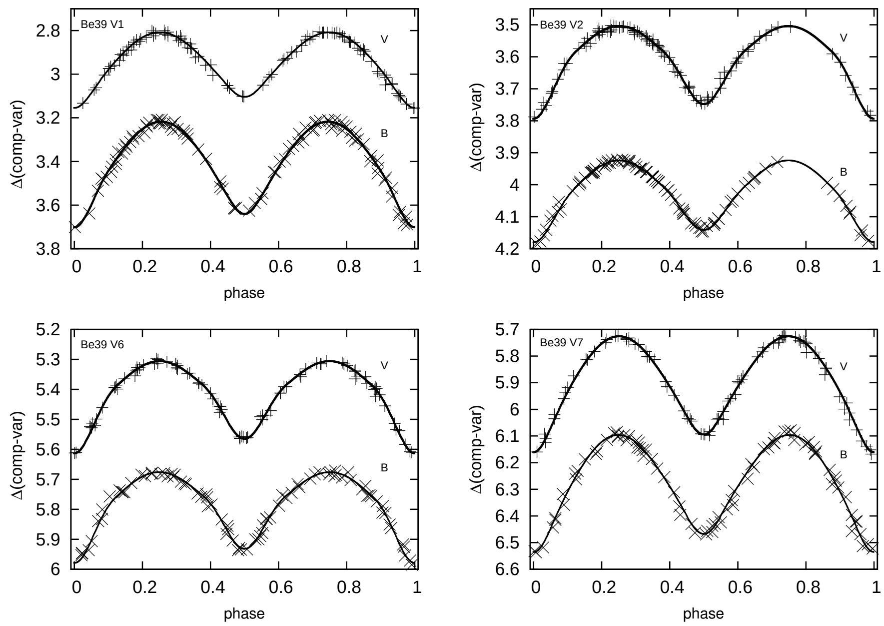

Fig. 4 Best fit in the V and B passband light curves of variables (V1, V2, V6 and V7). The points represent the observed data and the line marker represents the best fit.

5.2 Variable V2

The period of the system is $0.4865\mathrm{d}$ and $B-V=0.52$, which closely corresponds to the G1 spectral type. The combined result in the three bands shows a temperature difference of $\sim 270\,\mathrm{K}$ between the two components. The best combined values of q and i came out to be 0.79 and 61° respectively. The fill-out factor is 0.225 which is of intermediate level. The distance of the variable is around $4074\,\mathrm{pc}$.

5.3 Variable V6

The period of the system is $0.2844\mathrm{d}$ and $B-V=0.67$, which closely corresponds to the G4 spectral type. The combined result in the three bands shows a temperature difference of $\sim 300\,\mathrm{K}$ between the two components. The best combined values of q and i came out to be 0.78 and 64° respectively. The fill-out factor is 0.245, which is of intermediate level. The distance of the variable is around $4800\,\mathrm{pc}$.

5.4 Variable V7

The period of the system is $0.2780\mathrm{d}$ and $B-V=0.67$, which corresponds to the G4 spectral type. The combined result in the three bands shows a temperature difference of $\sim 200\,\mathrm{K}$ between the two components. The best combined values of q and i came out to be 1.17 and 66° respectively. The fill-out factor is 0.284, which is of intermediate level. The distance of the variable is around $5675\,\mathrm{pc}$.

5.5 Variable V8

The period of the system is $0.2288\mathrm{d}$ and $B-V=0.87$, which closely corresponds to the K2 spectral type. The maxima and minima of the light curves are almost equal in both the filters. The combined result in the three bands shows a temperature difference of $\sim 75\,\mathrm{K}$ between the two components. The

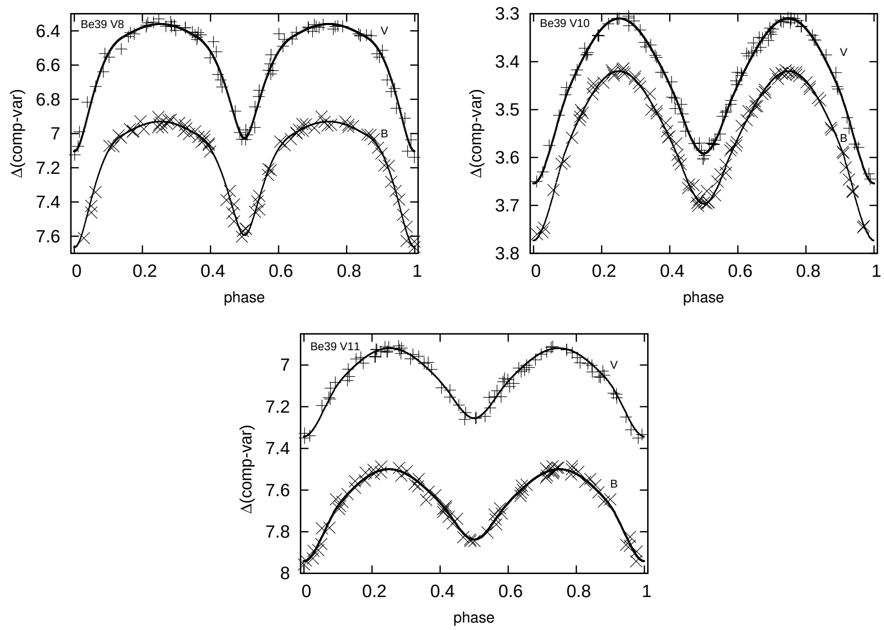

Fig. 5 Same as Fig. 4 but for variables V8, V10 and V11.

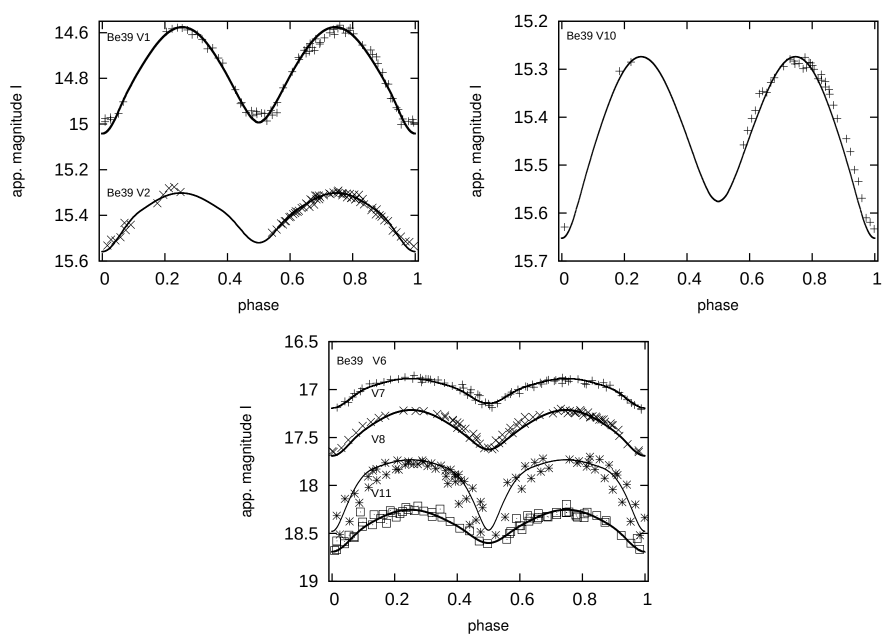

Fig. 6 Best fit in I passband light curves of observed variables. The symbols represent the observed data and the line marker represents the best fit.

Table 3 Combined Multi-color Photometric Elements Obtained for the Variables by Using the WD Code

Parameter	V1	V2	V6	V7	V8	V10	V11
Geometric Parameters							
Period (d)	0.4052	0.4865	0.2844	0.2780	0.2288	0.5419	0.2263
$\imath$ (°)	66.724 ±0.379	61.158 ± 0.265	64.117± 0.441	66.527 ±0.395	80.438 ± 0.687	63.118±0.208	65.223 ± 0.589
q	1.720 ±0.034	0.788 ± 0.017	0.779± 0.022	1.174 ±0.025	1.281 ± 0.108	1.301±0.018	1.251 ± 0.015
$\Omega_{1,2}$	4.635 ± 0.050	3.282 ± 014	2.977±0.028	3.830 ± 0.036	4.151 ± 0.169	4.052 ± 0.009	4.018 ± 0.027
Fill-out Factor	0.163	0.225	0.245	0.284	0.179	0.323	0.112
Fractional radii of star 1							
r_1							
POLE	0.323 ± 0.006	0.366 ± 0.005	0.367 ± 0.006	0.349 ± 0.005	0.325 ± 0.020	0.335 ± 0.001	0.345 ± 0.004
POINT	0.428 ± 0.004	0.453 ± 0.008	0.468 ± 0.003	0.463 ± 0.008	0.403 ± 0.017	0.438 ± 0.008	0.345 ± 0.004
SIDE	0.343 ± 0.008	0.456 ± 0.0019	0.385 ± 0.007	0.367 ± 0.006	0.338 ± 0.025	0.351 ± 0.001	0.362 ± 0.004
BACK	0.373 ± 0.016	0.410 ± 0.001	0.412 ± 0.010	0.404 ± 0.010	0.367 ± 0.037	0.383 ± 0.002	0.395 ± 0.007
Fractional radii of star 2							
r_2							
POLE	0.392 ± 0.005	0.323 ± 0.001	0.331 ± 0.006	0.375 ± 0.005	0.391 ± 0.019	0.378 ± 0.002	0.375 ± 0.003
POINT	0.427 ± 0.004	0.423 ± 0.008	0.435 ± 0.003	0.497 ± 0.008	0.482 ± 0.017	0.486 ± 0.008	0.474 ± 0.004
SIDE	0.417 ± 0.007	0.341 ±0.001	0.345 ± 0.008	0.396 ± 0.006	0.408 ±0.024	0.399 ± 0.001	0.395 ± 0.004
BACK	0.448 ± 0.001	0.404 ± 0.005	0.373 ± 0.011	0.425 ± 0.009	0.434 ± 0.033	0.429 ± 0.002	0.427 ± 0.006
Radiative Parameters							
Spec. Type	G0	G1	G4	G4	K2	F5	K3
T_1 (K)	6300	6250	5600	5600	5000	6800	4900
T_2 (K)	6065 ±87	5981 ±78	5302± 72	5399 ± 77	4925 ± 82	6210± 75	4630 ± 89
Luminosity Ratio							
L_1^B	0.4307	0.6253	0.6439	0.4884	0.4357	0.5576	0.5476
L_2^B	0.5693	0.3747	0.3561	0.5116	0.5643	0.4424	0.4524
L_1^V	0.4309	0.6244	0.6443	0.4890	0.4382	0.5580	0.5474
L_2^V	0.5691	0.3756	0.3557	0.5110	0.5618	0.4420	0.4526
L_1^I	0.4297	0.6267	0.6441	0.5042	0.4672	0.5578	0.5487
L_2^I	0.5703	0.3733	0.3559	0.4968	0.5328	0.4422	0.4513
$\sum$	0.0011	0.0030	0.0018	0.0035	0.0216	0.0032	0.0022

best combined values of q and i are 1.28 and $80°$ respectively. The temperature difference between the two components and the value of the fill-out factor (0.179) suggests that this system has good thermal contact but poor geometrical contact. The distance of the variable is around 4875 pc.

5.6 Variable V10

The period of the system is 0.5419d and $B - V = 0.41$, which corresponds to the F5 spectral type. The combined result shows a temperature difference of ~ 600 K between the two components. The best combined values of q and i are 1.30 and $63°$ respectively. The fill-out factor is found to be 0.323, which indicates a reasonably good geometrical contact of the system. The distance of the variable is around 4700 pc.

5.7 Variable V11

The period of the system is 0.2263d and $B - V = 0.88$, which corresponds to the K3 spectral type. The combined result in the three bands shows a temperature difference of $\sim 270\,\text{K}$ between the two components. The best combined values of q and i are 1.25 and 65° respectively. The fill-out factor of 0.112 is somewhat low for W UMa systems. This fill-out factor indicates that the stars of this system might have come into contact recently. The distance of the variable is around $6400\,\text{pc}$. This system may also be a field star that is in the background of the cluster.

6 DISCUSSION AND CONCLUSIONS

The photometric solutions suggest that all the variables are W-type systems of which five variables (V1, V7, V8, V10 and V11) have mass ratio greater than 1, and the remaining two (V2 & V6) have mass ratios less than 1. The absolute physical parameters for these variables, given in Table 4, are derived using the Kepler, Newton and Stefan-Boltzman laws provided by Gazeas (2009). We find that they do not show a large discrepancy with respect to field contact binaries. Gazeas & Niarchos (2006) showed that A-type systems would evolve into W-type systems because of the loss of total mass and AM. Gazeas & Stępień (2008) performed a detailed theoretical calculation of mass and AM loss via stellar wind from a detached binary evolving into a W-type W UMa system with shorter periods and low total mass, which agrees with our results. However, in their computed model results, the mass ratio in the coalescence configuration does not need to be low (Gazeas & Stępień 2008) which is contradictory to the conclusion of Li et al. (2008). Generally it is observed that A-type systems have low mass ratio values when compared to the mass ratios of W-type ones with few exceptions.

Table 4 Estimated Absolute Elements for Seven Variables

Variable	$M_1(M_\odot)$	$M_2(M_\odot)$	$R_1(R_\odot)$	$R_2(R_\odot)$	$L_1(L_\odot)$	$L_2(L_\odot)$
V1	1.155±0.025	1.987±0.008	1.086±0.010	1.370±0.008	0.974±0.053	1.556±0.033
V2	1.399±0.036	1.103±0.010	1.437±0.012	1.298±0.008	2.307±0.077	1.877±0.063
V6	0.949±0.024	0.739±0.007	0.874±0.007	0.785±0.007	0.596±0.092	0.480±0.028
V7	0.905±0.023	1.062±0.006	0.807±0.008	0.865±0.008	0.456±0.045	0.524±0.043
V8	0.781±0.023	1.000±0.005	0.665±0.005	0.740±0.005	0.266±0.092	0.330±0.021
V10	1.457±0.036	2.222±0.010	1.480±0.013	1.657±0.012	2.344±0.092	2.943±0.073
V11	0.776±0.026	1.138±0.005	0.661±0.006	0.727±0.005	0.262±0.025	0.318±0.023

1 – Primary, 2 – Secondary.

Li et al. (2008) found that the relationship between the mass ratio and the total mass of a contact binary system indicates that the high mass ratio systems evolve towards low mass ratio systems due to mass loss and AM loss mechanisms. The high mass ratio contact binary systems can be understood in the framework of the mass transfer process implying that mass transfer is taking place from the primary (more massive) to the secondary component (less massive), thus decreasing the period of the respective system. It is argued that the energy transfer is less for a higher evolutionary rate of the primary component (Liu & Yang 2000a,b). These results strongly indicate that in high mass ratio systems, the primary has a high degree of evolution and relative energy. Its mass transfer is less compared to the low mass ratio binaries.

Qian (2001) studied overcontact binaries and found that there exists a critical mass ratio ($q = 0.4$) where period increase ($q > 0.4$) or decrease ($q < 0.4$) occurs. According to TRO models (Lucy 1976; Flannery 1976; Robertson & Eggleton 1977), which are dependent on mass ratios and periods, contact binaries oscillate between contact and semi-detached systems due to the transfer of mass and energy. In the contact stage, the direction of mass transfer is opposite to that of the energy transfer and causes a rapid increase in separation. The system then reaches a configuration with the primary filling its lobe and transferring material to the secondary. In the TRO model the system oscillates around a marginal stable point. As the mass is transferred from the secondary to the primary component the system reaches a semi-detached stage with a low mass ratio and higher period. Later the mass transfer takes place from the primary to the secondary, decreasing the period and the mass ratio increases. This stage is the high end mass. Our solutions show that most of the observed variables have high end mass ratio values thus suggesting that all the member variables are at different stages in their TRO cycle. However, the sample was small and hence this kind of study should be extended to other contact binaries to confirm the real dependency of mass ratio and period change. Our study shows that all the variables have a mass ratio of > 0.4 and should have a trend of increasing period, i.e. the variables should evolve towards a semi-detached configuration. Incidentally, no such trend has been observed in these variables during the period 1993–2009. We found that the variables V1 and V2 have similar periods, $B - V$ values, and temperatures (T_1, T_2), but their mass ratios and luminosities differ in all the three passbands. Variables V6 and V7 also have similar values of periods, $B - V$, temperatures and the luminosities, but differ in their mass ratios. Variables V8 and V11 have similar values of period, $B - V$, temperatures and mass ratios, but differ in their luminosities. Therefore, the short period contact binaries (V6, V7, V8 and V11) are very important for future studies in order to discover their radiative and dynamical evolution and the period changes in these systems would be helpful to constrain the TRO model.

The photometric mass ratios of variables in Be 33, NGC 6791, Be39 and NGC 7789 suggest that most of them are W-subtype with mass ratio $q > 1$ or intermediate mass ratio values, independent of the respective cluster age (Rukmini & Vivekananda Rao 2002; Rukmini et al. 2005; Sriram et al. 2009; Sriram & Vivekananda Rao 2010). This work, along with our previous ones, suggests that the frequency of W-type systems is high compared to the frequency of A-type ones in clusters, which supports the theoretical evolutionary idea that A-type systems evolve into W-types. Gazeas & Stępień (2008) showed that binaries with periods 0.5–0.7 d have an age of about 5–6 Gyr but the studied variables have much shorter periods (except V10) which are probably members of the cluster with age ~ 6 Gyr. This indicates that the evolution of each variable is going through different phases or the mass and AM loss rate are high in order to have such low period contact binaries in a 6 Gyr old cluster. A possible candidate of excess loss of AM from the binary systems could show the presence of a third body. This possibility is also supported by the argument that a slight increase in mass transfer among the binary components results in a wider orbit (Gazeas & Stępień 2008) but most of the studied variables have periods less than 0.3 d. The other possibility is that short period variables in Be39 could have smaller orbital size in their pre-contact phase (less than 2 d, as assumed in Gazeas & Stępień 2008), and because of the average rate of mass and AM loss, such short period variables are observed.

Future photometric and spectroscopic observations would be useful to know the possible period changes and constrain the mass ratio of member variables and would also be important for understanding the evolutionary status of these systems.

Acknowledgements We thank the Director of IUCAA for allotting the observing time on the 2.0 m telescope. The authors acknowledge the anonymous referees for their useful comments.

References

Allen, C. W., & Cox, A. N. 2000, Allen's Astrophysical quantities (4th ed.; New York: Springer)
Binnendijk, L. 1970, Vistas in Astronomy, 12, 217
Diaz-Cordoves, J., Claret, A., & Gimenez, A. 1995, A&AS, 110, 329
Flannery, B. P. 1976, ApJ, 205, 217
Gazeas, K., & Stępień, K. 2008, MNRAS, 390, 1577
Gazeas, K. D. 2009, Communications in Asteroseismology, 159, 129

Gazeas, K. D., & Niarchos, P. G. 2006, MNRAS, 372, L83
Girardi, L., & Bertelli, G. 1998, MNRAS, 300, 533
Hilditch, R. W. 1989, Space Sci. Rev., 50, 289
Janes, K. A., Friel, E., Montgomery, K., Phelps, R., & Marschall, L. 1992, Mem. Soc. Astron. Italiana, 63, 283
Jiang, D., Han, Z., Wang, J., Jiang, T., & Li, L. 2010, MNRAS, 405, 2485
Kaluzny, J., Mazur, B., & Krzeminski, W. 1993, MNRAS, 262, 49
Kopal, Z. 1959, Close Binary Systems (The International Astrophysics Series, London: Chapman & Hall)
Kwee, K. K., & van Woerden, H. 1956, Bull. Astron. Inst. Netherlands, 12, 327
Li, L., Zhang, F., Han, Z., Jiang, D., & Jiang, T. 2008, MNRAS, 387, 97
Liu, Q., & Yang, Y. 2000a, A&AS, 142, 31
Liu, Q., & Yang, Y. 2000b, A&A, 361, 226
Lucy, L. B. 1967, ZAp, 65, 89
Lucy, L. B. 1976, ApJ, 205, 208
Mazur, B., Krzeminski, W., & Kaluzny, J. 1999, Acta Astronomica, 49, 551
Percival, S. M., & Salaris, M. 2003, MNRAS, 343, 539
Qian, S. 2001, MNRAS, 328, 914
Robertson, J. A., & Eggleton, P. P. 1977, MNRAS, 179, 359
Ruciński, S. M. 1969, Acta Astronomica, 19, 245
Rucinski, S. M. 1993, PASP, 105, 1433
Rucinski, S. M., & Duerbeck, H. W. 1997, PASP, 109, 1340
Rucinski, S. M. 1998, AJ, 116, 2998
Rucinski, S. M. 2000, AJ, 120, 319
Rukmini, J., Rao, P. V., & Sriram, K. 2005, Ap&SS, 299, 109
Rukmini, J., & Vivekananda Rao, P. 2002, Bulletin of the Astronomical Society of India, 30, 665
Sriram, K., Kiron, Y. R., & Vivekananda Rao, P. 2009, RAA (Research in Astronomy and Astrophysics), 9, 1149
Sriram, K., & Vivekananda Rao, P. 2010, RAA (Research in Astronomy and Astrophysics), 10, 159
van Hamme, W., & Wilson, R. E. 2003, in ASP Conf. Ser. 298, GAIA Spectroscopy: Science and Technology, ed. U. Munari, 323
Wilson, R. E., & Devinney, E. J. 1971, ApJ, 166, 605